HEFAT2012
9th International Conference on Heat Transfer, Fluid Mechanics and Thermodynamics
16 – 18 July 2012
Malta

NUMERICAL STUDY ON DESALINATED WATER FLUX FROM NACL SOLUTION USING HOLLOW FIBER TYPE DCMD MODULE

Jung-Gil Lee[a], Baek-Gyu Im[a] and Woo-Seung Kim[b]
[a*]Department of Mechanical Engineering, Hanyang University, 17 Haengdang-dong, Seongdong-gu, Seoul, Republic of Korea
[b]Author for correspondence
[b]Department of Mechanical Engineering, Hanyang University, 1271 Sa3-dong, Sangnok-gu, Ansan, Gyeonggi-do, Republic of Korea
E-mail: wskim@hanyang.ac.kr

ABSTRACT

The direct contact membrane distillation process is used for water desalination. DCMD is a thermally driven separation process, in which only vapor molecules transfer through a microporous hydrophobic membrane. The driving force in the DCMD process is the vapor pressure difference induced by the temperature difference across the hydrophobic membrane.

In this study, the one-dimensional based model is developed for predicting the performance of the seawater desalination to produce fresh water for hollow fiber type DCMD module. The mass, energy and momentum balance equations are coupled to determine the concentration of NaCl, the temperature and velocity distribution of the feed and permeate side along the module length, and productivity of fresh water in the DCMD process. The KMPT model is used to calculate the mass transfer at the membrane surface. The mathematical and kinetics models used in this study are validated in comparison of the present simulation results with previous data given in the literature. The simulation results are in good agreement with the data in the literature. The performance of pure water production rate with respect to the membrane distillation coefficient is compared with the previously reported data.

The numerical analysis is performed on a DCMD module using hollow fiber type PVDF membrane with a pore size of 0.22 µm. Feed solutions are aqueous NaCl solution. The values of the parameters considered in this work are: feed temperature, 40-70℃; feed velocity, 0.472m/s to 0.55m/s; mass fraction of salt, 0.025-0.05; cold permeate temperature, 17-45℃ and the velocity of the permeate side are 0.3 m/s. It is found that the production rate of fresh water increases with feed temperature and velocity, but decreases with feed concentration.

INTRODUCTION

Membrane distillation(MD) is a promising technology for producing highly pure water. The potential advantages of the MD process are lower operating temperature, hydrostatic pressure and insensitivity to salt concentration. However, one of the major disadvantages of MD is its relatively low permeate flux compared to other separation techniques, such as reverse osmosis. Therefore, MD process required to properly design a module with a very high effective area. Hollow fiber type membrane devices for MD process are simple, potentially scalable, and they can often pack a large membrane surface area per unit volume of the device.

Direct Contact Membrane Distillation(DCMD) is a thermally driven process by a vapor pressure gradient across a hydrophobic microporous membrane, which blocks between a hot feed solution and a cold permeate side. The hydrophobic membrane prevents any liquid from entering the pores. The temperature difference between the hot feed solution and cold permeate sides is the main factor that creates the driving force for DCMD mass transfer. As the process is non-isothermal, vapor molecules will move through the membrane pores form the high to the low vapor pressure side.

Many previous researches on DCMD have employed hollow fiber membrane modules. Gryta and Tomaszewska [2] presented and verified the heat transport in DCMD capillary modules. Lagana et al. [3] shows a model of tubular membrane for the effect evaluation of membrane morphology, such as thickness, elastic modules and pore radius distribution on permeate flux. Lie and Sirkar [4] presented a remarkable high water vapor flux up to $79 kgm^{-2}h$ and high module productivity. Schneider et al. [5] pointed out that only the wetting pressure, i.e. the liquid entry pressure of the feed solution into the membrane pores, should be no less than 250kPa to ensure sufficient safety tolerance with respect to pressure fluctuations and temperature increases. Phattaranawik et al. [8] presented a model based on the linear temperature profile through the membrane. This presented model was able to study the effect of mass transfer on heat transfer rates and heat transfer coefficients.

In the present work, systematical model equations for DCMD based desalination through countercurrent hollow fiber module are made from mass, momentum and energy balance of both feed and permeate sides as well as the flux across the membrane during the inlet feed temperature (20-70℃), inlet permeate temperature(17-45℃), inlet feed velocity(0.472-0.55m/s), inlet permeate velocity (0.3m/s) and mass fraction of salt (0.025-0.05).

NOMENCLATURE

A	[m^2]	Membrane area ratio for heat transfer through fiber outside, fiber wall or fiber inside.
C	[kg/m^2hrpa]	Membrane distillation coefficient
C_K	[-]	Individual Contribution of Knudsen diffusion to MD coefficient
C_M	[m^{-1}]	Individual contribution of Molecular diffusion to MD coefficient
C_{Pf}	[m]	Individual contribution of Poiseuille flow to MD coefficient
C_p	[J/molK]	Specific heat
d	[m]	Diameter of fiber
dh	[m]	Hydraulic diameter
d_i	[m]	Inside diameter of fiber
d_o	[m]	Outside diameter of fiber
d_s	[m]	Inside diameter of shell (m)
D	[m]	Diffusion coefficient(m2s)
h	[$wm^{-2}K^{-1}$]	Convective heat transfer coefficient
ΔH	[Jkg^{-1}]	Enthalpy of water evaporation
J	[$kgm^{-2}h^{-1}$]	Mass vapor flux
k	[$wm^{-1}K^{-1}$]	Thermal conductivity coefficient
L	[m]	Module length
M	[$g\ mol^{-1}$]	Molecular weight(g mol^{-1})
N	[-]	Number of fibers
P	[Pa]	Pressure
PR	[$kg\ m^{-2}$]	Productivity
Q	[w]	Heat energy
R	[$Jmol^{-1}K^{-1}$]	Ideal gas constant
R_K	[-]	Correlation form of Knudsen diffusion
R_M	[-]	Correlation form of Molecular diffusion
R_{Pf}	[-]	Correlation form of Poiseuille diffusion
T		temperature(K)
x		molar fraction in liquid phase
v		velocity(ms-1)
V		molar volume, (m3mol-1)
Z		axial coordinate for hollow fiber

Dimensionless numbers

Nu	Nusselt number
Pr	Prandtl number
Re	Reynolds number

Greek letters

α	[-]	Membrane surface area based on fiber inside diameter per unit length per fiber layer.
δ	[m]	Membrane thickness(m)
ε	[m]	Membrane porosity
μ	[Pa s]	Kinematic viscosity
ρ	[kg/m^3]	Density
Φ		packing density
X		membrane pore tortuosity

Subscripts

b	Bulk
s	Salt
w	Water
m	Membrane

Superscripts

F	Feed side
P	Permeate side

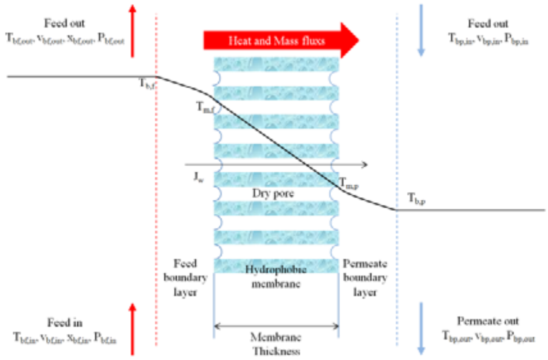

Figure 1 Mass and heat transfers during MD

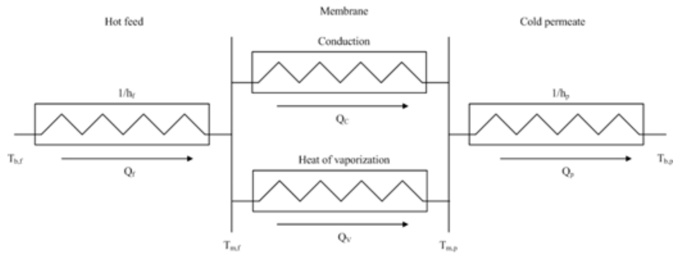

Figure 2 Thermal circuit analogy of heat transfer resistances in DCMD.

MATERIALS

A durable GVSP(PVDF, pore size of 0.2 m, thickness of 125mm, Millipore) hydrophobic membrane was used as a substrate membrane in hollow fiber type module. The feed liquids employed in DCMD numerical analyses were distilled water and mass fraction of NaCl solution(0.025-0.05), for the separation numerical analyses.

MEMBRANE FLUX

The module of hollow fiber type DCMD consists of three layers including the tube feed side, the membrane layer and the shell cold permeate side.

DCMD process is in described four steps as follows: (1) the heat and volatile solution from the bulk of hot feed side flow on the membrane surface, (2) the volatile solution from the liquid-vapor interface evaporate on the feed side of the membrane surface and absorption of latent heat, (3) water vapor diffuse through the membrane and heat conduct across the membrane, (4) water vapor condense on the permeate side of the membrane and release the latent heat. The physical processes in DCMD membrane are depicted in **Figure 1.**

The main assumptions used in this study are as follows: (1)Steady incompressible flow, (2)Negligible heat loss to atmosphere, (3)The fibers distributed evenly and regularly within the shell of the module, and (4)No friction for the feed in tube.

HEAT TRANSFER

The heat transfer involved in DCMD can be divided into three regions as shown in **Figure 2**:

(1) within the boundary of the tube feed side.

$$Q^F = h^F A_r^F \alpha \, (T^F - T_m^F) \quad (1)$$

Where, T^F and T_m^F are the temperatures of the bulk feed and at the feed side of the membrane, respectively. The heat transfer coefficient in the tube side h^F is chosen from the following equations(2a, 2b).

$$Nu^F = \frac{h^F d_h}{k^F} = 1.86\left(\mathrm{Re}^F \, \mathrm{Pr}^F \frac{d_h}{L} \right)^{0.33} \left(\frac{\mu_s}{\mu_w} \right)^{0.33} \quad (2a)$$

$$\mathrm{Re}^F = \frac{d_s v_s \rho_s}{\mu_s}; \quad \mathrm{Pr}^F = \frac{C_{ps}\mu_s}{k_s} \quad (2b)$$

(2)Within the boundary of the cold permeate side.

$$Q^P = h^P A_r^P \alpha \, (T_m^P - T^P) \quad (3)$$

Where, T_m^P and T^P are the temperatures at the permeate side of the membrane and the cold bulk, respectively. The heat transfer coefficient in cold permeate side could be described in equations(4a, 4b).

$$Nu^P = \frac{h^P d_h}{k^P} = 1.86\left(\mathrm{Re}^P \, \mathrm{Pr}^P \frac{d_h}{L} \right)^{0.33} \left(\frac{\mu_w}{\mu_w} \right)^{0.33} \quad (4a)$$

$$\mathrm{Re}^P = \frac{d_w v_w \rho_w}{\mu_w}; \quad \mathrm{Pr}^P = \frac{C_{pw}\mu_w}{k_w} \quad (4b)$$

(3) across the membrane.

$$Q^m = A_{rm}\alpha \left[J\Delta H + \frac{k_m}{\delta_m} \, (T_m^F - T_m^P) \right] \quad (5)$$

$$A_{rm} = \left(\frac{d_{lm}}{di} \right), \quad d_{lm} = \frac{d_o - d_i}{\ln(d_o / d_i)} \quad (6)$$

where, J is the transmembrane mass flux. δ_m is the membrane thickness. $k_m = \varepsilon k_{mg} + (1-\varepsilon)\, k_{ms}$, where ε is the membrane porosity. k_{mg} and k_{ms} refer to the conductive coefficients of vapor within the membrane pore and the solid membrane, respectively. At the steady state, the amount of heat transferred through the boundaries of both fluids is equal to that across the membrane; thus Equations.(1), (3) and (5) satisfy.

$$Q^F = Q^m = Q^P \quad (7)$$

MASS TRANSFER

In the DCMD process, the mass transport is usually described by assuming a linear proportion between the mass flux(J) and the water vapor pressure difference through the membrane distillation coefficient(C).

$$J = C \, (P_m^F - P_m^P) \quad (8)$$

Where C is the mass transfer coefficient, P_m^F and P_m^P are the water vapor pressures on the feed and the permeate sides of the membrane surface, respectively. The water vapor pressure is calculated using the antoine equation at the temperatures T_m^F and T_m^P, respectively such as following:

$$P_m = \exp\left(23.328 - \frac{3841}{T - 45} \right) \quad (9)$$

Since there is dissolved species with the molar concentration x_s^F at the feed side, the reduction in the vapor pressure can be described according to Raoult's law.

$$P_m^F = P_m^w \, (1 - x_s^F) \quad (10)$$

Where, $P^W{}_m$ refers to the vapor pressure when there is no dissolved species in the water.

Since the mean free molecular path of the water vapor under the DCMD operating conditions is comparable to the typical pore size used in the MD membrane, more than one mechanism of mass transport simultaneously occur because of the pore distribution of the membranes. The hybrid model of Knudsen diffusion-Molecular diffusion- Poiseuille flow transition called KMPT model is used[6]. Thus, the membrane distillation coefficient is showed by

$$C = (R_K + R_M)^{-1} + R_{Pf}^{-1} \quad (11)$$

where $R_K^{-1} = C_K(M_W/RT_m)^{0.5}$, $R_M^{-1} = C_M(DM_W/P_{aM}RT_m)$, and $R_{Pf}^{-1} = C_{Pf}(P_m M_W/\mu RT_m)$, C_K, C_M, and C_{Pf} represents the individual contribution of Knudsen diffusion, Molecular diffusion and Poiseuille flow, respectively, the values of which are given in **Table 1**.

TRANSPORT MODELS OF FEED AND PERMEATE SIDES

The permeate flux J depends on operation conditions existing on both sides: feed side and permeate side of the membrane surface. A schematic representation of the typical flow pattern in a hollow fiber module with feed side and the countercurrent permeate stream is described in **Figure 1.**

(1)Hot brine feed side

On the basis of the momentum, mass and energy balances for the hot brine feed side, the following equations in terms of pressure(P^F), velocity(v^F), compositions(x_s^F), and temperature(T^F) are derived. The derivations of the model equations are listed.

$$\frac{dP^F}{dz} = -\frac{32\mu^F}{d_i^2} v^F \tag{12}$$

$$\frac{1}{V^F}\frac{dv^F}{dz} - \frac{v^F}{(V^F)^2}\left(\frac{M_s}{\rho_s} - \frac{M_w}{\rho_w}\right)\frac{dx_s^F}{dz} = -\frac{4Jd_o}{M^F d_i} \tag{13}$$

$$\frac{x_s^F}{V^F}\frac{dv^F}{dz} + \frac{M_w v^F}{\rho_w (V^F)^2}\frac{dx_s^F}{dz} = 0 \tag{14}$$

$$\frac{d\rho^F v^F C_p^F T^F}{dz} = \frac{-4Q^F}{\pi N d_i^2} \tag{15}$$

where, V^F is the feed molar volume. M_s, M_w and M^F are the molecular weight of salt, water and feed.

(2)Cold permeate side

In the permeate side, the momentum , mass and energy balances provide coupled differential equations in terms of pressure(P^P), velocity(v^P), and temperature(T^P). Where the composition term is neglected due to the near 100% rejection of non-volatile ionic solutes in DCMD of desalination.

$$\frac{dP^P}{dz} = \frac{32\mu^P}{d_h^2} v^P \tag{16}$$

$$\frac{dv^P}{dz} = -\frac{4V^P NJd_o}{M^P\left(d_s^2 - Nd_o^2\right)} \tag{17}$$

$$\frac{d\rho^P v^P C_p^P T^P}{dz} = \frac{-Q^P}{d_s^2 - Nd_o^2} \tag{18}$$

Related variables are similar to those variables in the feed side, but the superscript is for the permeate side. The boundary conditions :

For the hot brine water feed side

$$T(0) = T_{in}^F,\ \ v(0) = v_{in}^F,$$

$$x_s^F(0) = x_{s,in},\ P^F(L) = P^0 \tag{19}$$

For the cold permeate side

$$T(L) = T_{in}^P,\ \ v(L) = v_{in}^P,\ \ P^P(0) = P^0 \tag{20}$$

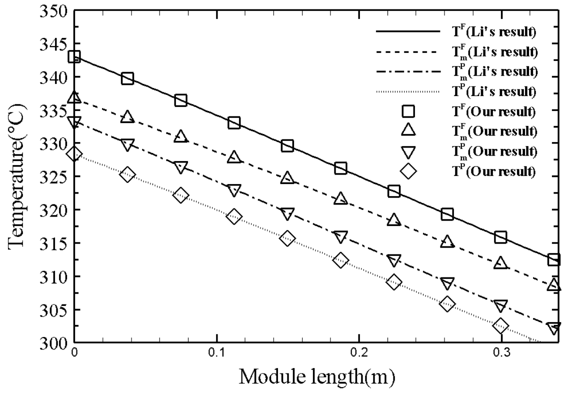

Figure 3 Temperature as functions of the fiber length (T_{in}^F =70℃, T_{in}^P =25℃, v_{in}^F= v_{in}^P =0.472m/s, w_{in}^F =0.025, Φ=0.6)

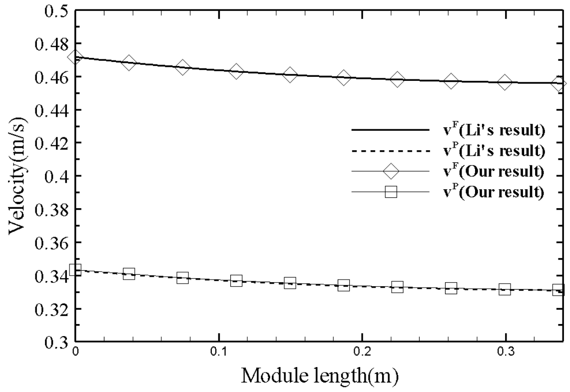

Figure 4 Velocity as a function of the fiber length (T_{in}^F =70℃, T_{in}^P =25℃, v_{in}^F= v_{in}^P =0.472m/s, w_{in}^F =0.025, Φ=0.6)

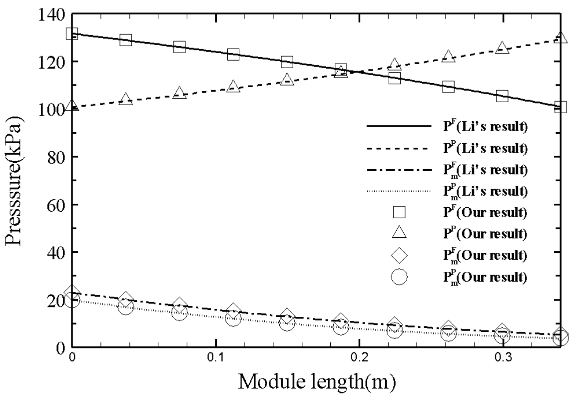

Figure 5 Pressure as a function of the fiber length (T_{in}^F =70℃, T_{in}^P =25℃, v_{in}^F= v_{in}^P =0.472m/s, w_{in}^F =0.025, Φ=0.6)

where the P^0 is equal to the ambient atmospheric pressure at both outlets of the fluids. The hollow fiber type membrane module parameters used for the simulation are given in **Table 1**.

Table 1 Characteristics of the membrane module

Hollow fiber membrane module	PVDF
Length of fibers(L, m)	0.34
Shell diameter(d_s, m)	0.03
Number of fibers(N)	3000
Inner diameter of fibers(d_i, mm)	0.3
Membrane thickness(δ_m, thickness)	60
Packing density(Φ,%)	60
C_K	$15.18X10^{-4}$
C_M	$5.1X10^{3}$
C_{Pf}	$12.97X10^{-11}$

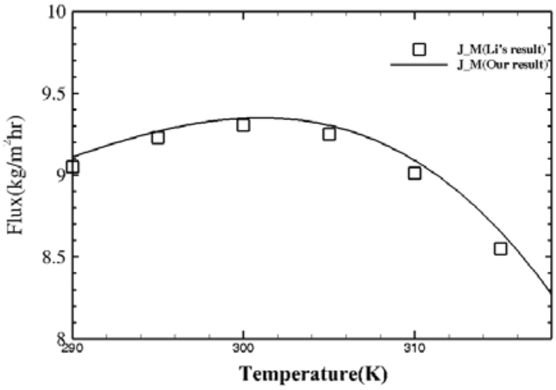

Figure 6 The effect of the inlet cold temperature on the mean permeate flux(T_{in}^F =70℃, v_{in}^F= v_{in}^P =0.472m/s, w_{in}^F =0.025, Φ=0.6)

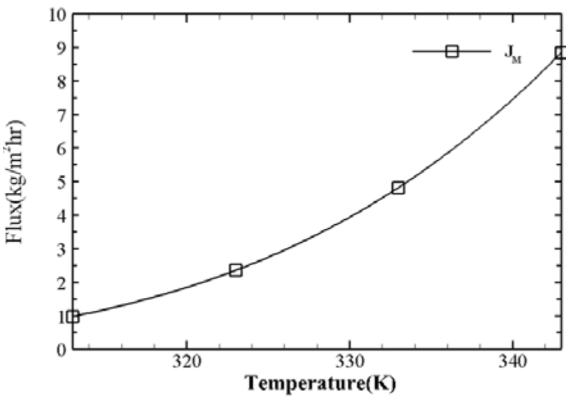

Figure 7 The effect of the inlet feed temperature on the mean permeate flux(T_{in}^P =17℃, v_{in}^F=0.472m/s, v_{in}^P =0.3m/s, w_{in}^F =0.025, Φ=0.6)

VALIDATED PREVIOUS EXPERIMENTAL AND NUMERICAL DATA

Property values of hollow fiber module type DCMD parameters for numerical simulations are shown in **Table 1.** As shown **Figure 3**, **Figure 4**, **Figure 5,** and **Figure 6** the numerical results were in good quantitative agreement with previous

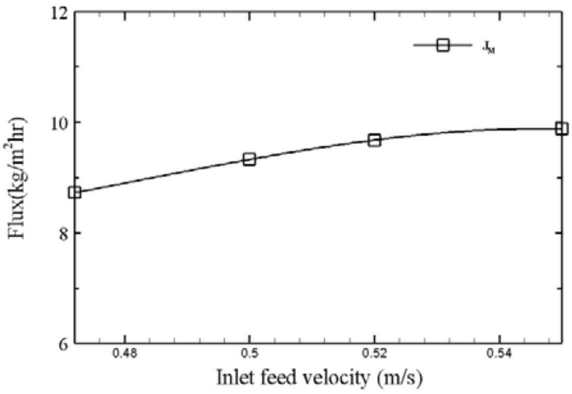

Figure 8 The effect of the inlet feed flow rate on the mean permeate flux(T_{in}^F =70℃, T_{in}^P =17℃, v_{in}^P =0.3m/s, w_{in}^F =0.025, Φ=0.6)

results[1].

EFFECT OF COLD PERMEATE SIDE TEMPERATURE

Figure 6 shows that J_M increases as T_{in}^P increases. But the results are apparently different from the general observation that permeate flux increases at lower cold temperature obtained from the flat sheet type module[7]. Maximum J_M result is 9.3 kg/m^2h at the inlet temperature of cold permeate side water of 30℃. Transmembrane vapor pressure based on the antoine equation is not only the exponential change in T_{in}^F but also the function of the transmembrane temperature $\Delta T= T_{in}^F - T_{in}^P$. It is possible that the transmembrane vapor pressure difference at the higher and the lower T_{in}^P are equal to each other when ΔT is relatively smaller whereas T_{in}^F is maintained at relatively higher values in the case of higher T_{in}^P. Therefore, lower T_{in}^P may not increase J_M as shown in **Figure 6**.

EFFECT OF HOT BRINE FEED SIDE TEMPERATURE

Figure 7 shows the J_M increases as T^F_{in} increases. The maximum permeate flux is 8.85 kg/m^2hr at the inlet hot brine temperature of 70℃. The exponential increase of permeate flux J_M is due to the water vapor pressure difference ΔP_m which is calculated by the antoine equation.

EFFECT OF HOT BRINE FEED SIDE FLOW RATE.

Figure 8 shows that J_M increases as feed flow rate increases, but the slopes gradually decreases at the higher feed flow rate. The maximum permeate flux is 9.8 kg/m^2hr at the inlet hot brine velocity of 0.55 m/s. The effect of feed velocity can increase the heat transfer coefficient and then reduce the temperature of feed solution. On the other hand, because of the shorter retention time of the stream within the hollow fiber module, the higher transmembrane temperature difference is

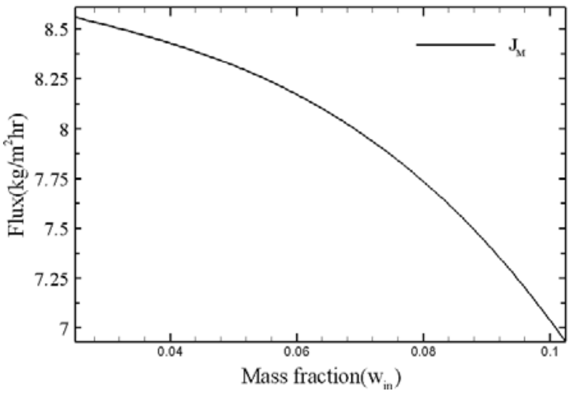

Figure 9 The effect of the inlet concentration of NaCl on the mean permeate flux(T_{in}^F =70℃, T_{in}^P =17℃, v_{in}^F=0.472m/s , v_{in}^P=0.3m/s, Φ=0.6)

maintained along the fiber length. Therefore, the high feed flow rate can increase to J_M.

EFFECT OF HOT BRINE FEED SIDE SODIUM CHLORIDE CONCENTRATION

Figure 9 shows that J_M decrease exponentially along the increasing of mass fraction of NaCl in the feed side. At a mass fraction of 0.025 which was closed to saturation and permeate flux is 8.55 kg/m^{2}hr. The minimum permeate flux is 6.73 kg/m^{2}hr at the mass fraction of 0.1025.

CONCLUSIONS

Direct contact Membrane by means of a composite membrane with a hydrophilic layer was developed for desalination. The mass, energy and momentum balance equations are coupled to determine the concentration of NaCl, the temperature and velocity distribution of the feed and permeate side along the module length, and productivity of fresh water in the DCMD process. In this paper, the DCMD numerical model is showed to investigate property variations of feed and permeate sides in a desalination system during DCMD.

The temperature of inlet hot brine solution decreases from the inlet 70 ℃ to the outlet 30 ℃, while temperature of inlet cold permeate side increases from inlet 25 ℃ to the outlet 58 ℃. The feed and permeate side temperature difference is constant throughout the membrane module by the counter-current pattern flow.

There is a velocity variation along the fiber length axial positions. The feed side velocity decreases from the inlet 0.472 m/s to the outlet 0.455 m/s while the permeate side velocity increases from the inlet 0.332m/s to the outlet 0.343m/s by the countercurrent flow pattern. The velocity variations of both solid of NaCl and permeate flux are not big enough, however, they have effect on the heat transfer on the membrane.

Variation of bulk pressure has no influence on the permeate flux, because the DCMD driving force is the water vapor pressure difference between both membrane surface sides. However, it is related with the variation of feed and permeate velocity along the module length.

The permeate flux increase with the increase of the temperature of feed hot brine solution, the velocity of feed hot brine water and the decrease of the mass fraction.

As shown in this paper, it is necessary to optimize operation conditions so that the performance can be optimized in the hollow fiber direct contact membrane distillation system for the desalination. The energy consumption and optimal design of DCMD system will be investigated in our future work.

ACKNOWLEDGMENTS

This work was supported by the Second Brain Korea 21 Project in 2012.

REFERENCES

[1] Cheng L.H, Wu P.C, Kong C.K and Chen J.H., Spatial variations of DCMD performance for desalination through countercurrent hollow fiber modules, *Desalination*, Vol.234, 2008, pp.323-334
[2] Gryta M and Tomaszewska M., Heat transport in membrane distillation process, *Journal of membrane science*, Vol.144, 1998, pp.211-222.
[3] Lagana F, Baribieri G, and Drioli E., Direct contact membrane distillation: modeling and concentration experiments, *Journal of membrane science*, Vol.166, 2000, pp.1-12.
[4] Li B and Sirkar K.K., Novel membrane and device for direct contact membrane distillation based desalination process, *Industrial and engineering chemistry research*, Vol.43, 2004, pp. 5300-5309.
[5] Schneider K, Holz W and Wollbeck R, Membranes and modules for transmembrane distillation, *Journal of membrane science*, Vol.39, 1988, pp.25-42.
[6] Ding Z, Ma R and Fane A.G, A new model for mass transfer in direct contact membrane distillation, *Desalination,* Vol. 151, 2002, pp.217-227.
[7] El-Bourawi M.S, Ding Z, Ma R and Khayet M., A framework for better understanding membrane distillation separation process, *Journal of membrane science*. Vol. 285, 2006, pp.4-29.
[8] Phattaranawik J, Jiraratananon R, and Fane A.G, Heat transport and membrane distillation coefficients in direct contact membrane distillation, *Journal of membrane science*, Vol.212, 2003, pp.177-193.